# Numerical investigation of drag reduction in turbulent channel flow by rigid fibers using a direct Monte-Carlo method

Amin Moosaie and Michael Manhart

Fachgebiet Hydromechanik
Technische Universität München

EUROMECH Colloquium 513
Dynamics of non-Spherical Particles in Fluid Turbulence

April 6-8, 2011

# Drag reduction by long-chain hydrocarbon polymer

Trans-Alaska Pipeline System (crude oil)

- Length: 800 miles
- Makes use of Toms effect (1948)
- Throughput without DR: 1.44 million barrels per day
- Throughput with DR: 2.13 million barrels per day

www.alyeska-pipe.com

# Outline

# Known features of polymeric/fibrous drag-reduced turbulent flows

- Increased spacing and coarsening of streamwise streaks
- Enhanced streamwise turbulence intensity
- Reduced spanwise and wall-normal turbulence intensities
- Reduced Reynolds shear stress
- Parallel shift of log-law in LDR, increase of its slope in HDR
- Damping of turbulence small scales
- Reduced streamwise vorticity fluctuations

Streaks at $z^+ = 7.5$

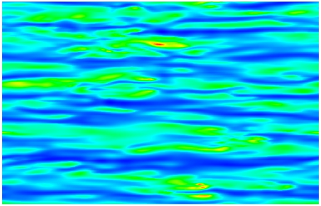

Newtonian flow

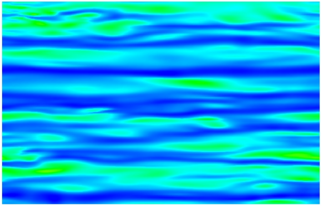

Drag-reduced flow

# Previous works on fiber-induced drag reduction (examples)

1. Rheological studies
   - Jeffery (1922): ellipsoidal particle in creeping flow
   - Batchelor (1970): stress in particle suspensions
   - Brenner (1974): rheology of dilute Brownian fiber suspensions

2. Experimental study
   - Paschkewitz et al. (2005): ZPG boundary layer

3. Numerical studies
   - den Toonder et al. (1997): pipe flow, simplifies model
   - Manhart (2003): channel flow, one-way coupled, Monte-Carlo
   - Paschkewitz et al. (2004): channel flow, closure model
   - Paschkewitz et al. (2005): ZPG boundary layer, closure model
   - Gillissen et al. (2008): channel flow, closure model and F-P eq.

• Not yet been done: direct Lagrangian simulation at high *Pe* in a big channel.

# Fiber geometry and assumptions

- Fiber geometry: prolate spheroid
- Orientation: unit axial vector **n**
- Aspect ratio: $r = L/D$ ($r \to \infty$ for slender fibers)
- A1 $L << \eta$
- A2 $\rho_p = \rho_f$
- A3 Dilute suspension

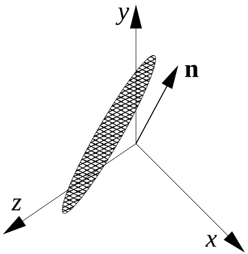

# Carrier flow field

- Above assumptions $\Rightarrow$ effect via non-Newtonian stress
- Incompressible non-Newtonian Navier-Stokes equations:

$$\boldsymbol{\nabla} \cdot \mathbf{U} = 0$$

$$\rho \frac{D\mathbf{U}}{Dt} = -\boldsymbol{\nabla} p + \boldsymbol{\nabla} \cdot \left( \boldsymbol{\tau}^{\mathrm{N}} + \boldsymbol{\tau}^{\mathrm{NN}} \right)$$

$$\boldsymbol{\tau}^{\mathrm{N}} = 2\mu\mathbf{D} \qquad \text{Newtonian stress tensor}$$

$$\boldsymbol{\tau}^{\mathrm{NN}} \qquad \text{non-Newtonian stress tensor}$$

# Non-Newtonian stress tensor

- Non-Newtonian stress depends on the orientation distribution of fibers (Brenner, 1974):

$$\boldsymbol{\tau}^{\mathrm{NN}} = 2\mu_0 \mathbf{D} + \mu_1 \mathbf{1}\left(\mathbf{D} : \langle \mathbf{nn} \rangle\right) + \mu_2 \mathbf{D} : \langle \mathbf{nnnn} \rangle$$
$$+ 2\mu_3 \left(\langle \mathbf{nn} \rangle \cdot \mathbf{D} + \mathbf{D} \cdot \langle \mathbf{nn} \rangle\right) + 2\mu_4 D_r \left(3 \langle \mathbf{nn} \rangle - \mathbf{1}\right)$$

- Moments of the orientation distribution function:

$$\langle \cdots \rangle = \oiint_{\mathbf{S}} \cdots \; \Psi\left(\mathbf{n}\right) \mathrm{d}S(\mathbf{n})$$

- $\mu_i = \mu_i\left(\mu, \phi, r\right)$: material coefficients
- $D_r$ : Brownian diffusivity

# Fiber orientation

- Fiber orientation distribution due to
  1. Carrier flow field
  2. Brownian motion
- Fokker-Planck equation:

$$\frac{D\Psi}{Dt} = \frac{\partial \Psi}{\partial t} + \mathbf{U} \cdot \boldsymbol{\nabla} \Psi = -\boldsymbol{\nabla}_{\mathbf{n}} \cdot (\Psi \dot{\mathbf{n}}) + \Delta_{\mathbf{n}} (D_r \Psi),$$

$$\dot{\mathbf{n}} = \boldsymbol{\Omega} \cdot \mathbf{n} + \kappa (\mathbf{D} \cdot \mathbf{n} - \mathbf{D} : \mathbf{nnn}) \quad \cdots \text{ Jeffery eq.,}$$

$$\mathbf{D} = \frac{1}{2} (\boldsymbol{\nabla} \mathbf{U} + \mathbf{U} \boldsymbol{\nabla}) \quad \cdots \text{ strain-rate,}$$

$$\boldsymbol{\Omega} = \frac{1}{2} (\boldsymbol{\nabla} \mathbf{U} - \mathbf{U} \boldsymbol{\nabla}) \quad \cdots \text{ rotation-rate.}$$

- High-dimensional problem!

# Solution algorithm

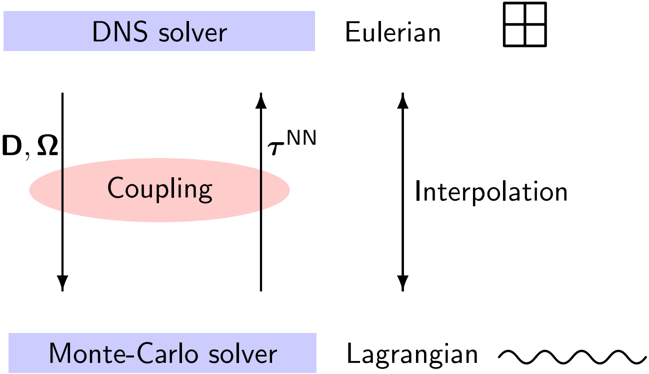

# DNS solver (MGLET)

- 3D unsteady incompressible Navier-Stokes equations
- Based on the projection method
- Finite volume method for spatial discretization
- Third-order Runge-Kutta scheme for time integration
- SIP iterative solver for the Poisson equation
- Cartesian non-equidistant grid
- Staggered arrangement of variables

# Monte-Carlo solver

- Ensemble of $N_f$ samples
- $i$-th sample is a stochastic process:

$$\mathrm{d}\mathbf{n}_i = \mathbf{A}\left(\mathbf{n}_i, t\right)\mathrm{d}t + B\left(\mathbf{n}_i, t\right)\mathrm{d}\mathbf{W}_i$$

$$\begin{aligned}\mathbf{A}\left(\mathbf{n}_i, t\right) &= \boldsymbol{\Omega}\cdot\mathbf{n}_i + \kappa\left(\mathbf{D}\cdot\mathbf{n}_i - \mathbf{D}:\mathbf{n}_i\mathbf{n}_i\mathbf{n}_i\right),\\ B\left(\mathbf{n}_i, t\right) &= \sqrt{2D_r},\end{aligned}$$

$\mathrm{d}\mathbf{W}_i$ increment of a 3D Wiener process.

- Monte-Carlo integration using $N_f$ samples:

$$\langle\mathbf{nn}\rangle \approx \frac{1}{N_f}\sum_{i=1}^{N_f}\mathbf{n}_i\mathbf{n}_i, \quad \langle\mathbf{nnnn}\rangle \approx \frac{1}{N_f}\sum_{i=1}^{N_f}\mathbf{n}_i\mathbf{n}_i\mathbf{n}_i\mathbf{n}_i$$

# Coupling

- DNS solver $\rightarrow$ Monte-Carlo solver
  - $\mathbf{D}$ and $\boldsymbol{\Omega}$ in Eulerian frame computed using fourth-order differentiation
  - $\mathbf{D}$ and $\boldsymbol{\Omega}$ transferred from Eulerian to Lagrangian frame using third-order interpolation
- Monte-Carlo solver $\rightarrow$ DNS solver
  - $\boldsymbol{\tau}^{\mathrm{NN}}$ from Lagrangian to Eulerian frame by cell averaging

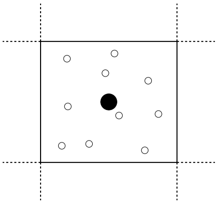

$$\boldsymbol{\tau}^{\mathrm{NN}} = \frac{1}{N_c} \sum_{i=1}^{N_c} \boldsymbol{\tau}_i^{\mathrm{NN}}$$

# Solution algorithm

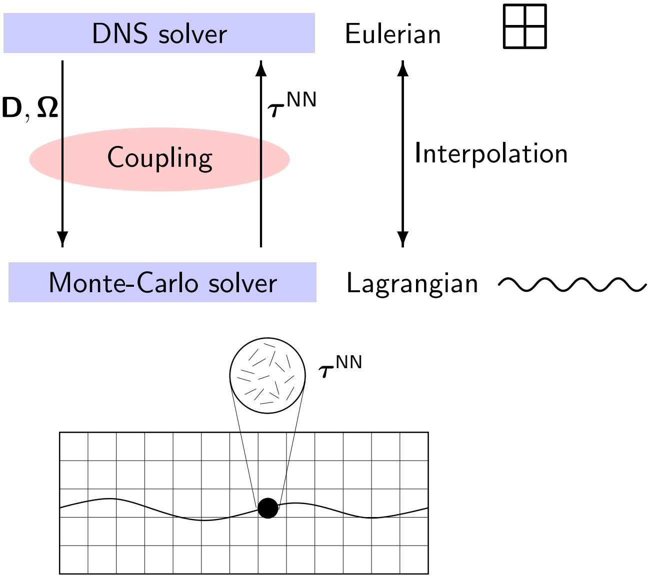

# Simulation parameters

- Turbulent channel flow at $\mathrm{Re}_\tau = 180$
- Concentration parameter $nL^3 = 18$
- Fiber aspect ratio $r = 100$
- Rotary Péclet number: $Pe_r = U_b/(hD_r) = 1000$
- Number of Lagrangian paths: $6.4 \times 10^7$
- Number of sampling fibers per Lagrangian path: 100
- Total number of fibers: $6.4 \times 10^9$
- Number of processors: 128 on SGI-Altix
- About 24 CPU seconds per time step
- Computational domain and grid:

| $L_x$ | $L_y$ | $L_z$ | $N_x$ | $N_y$ | $N_z$ | $\Delta x^+$ | $\Delta y^+$ | $\Delta z^+_{\min}$ |
|---|---|---|---|---|---|---|---|---|
| $3\pi h$ | $2\pi h$ | $2h$ | 128 | 128 | 128 | 13.25 | 8.84 | 0.675 |

# Mean velocity profile

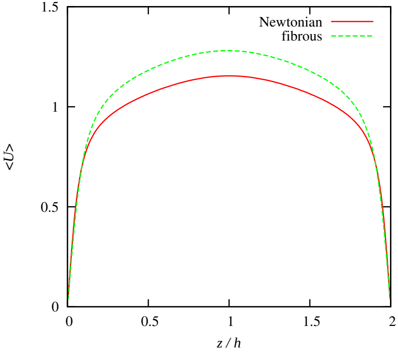


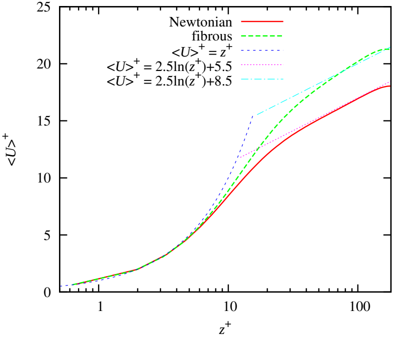

# Turbulence intensities and Lumley anisotropy map

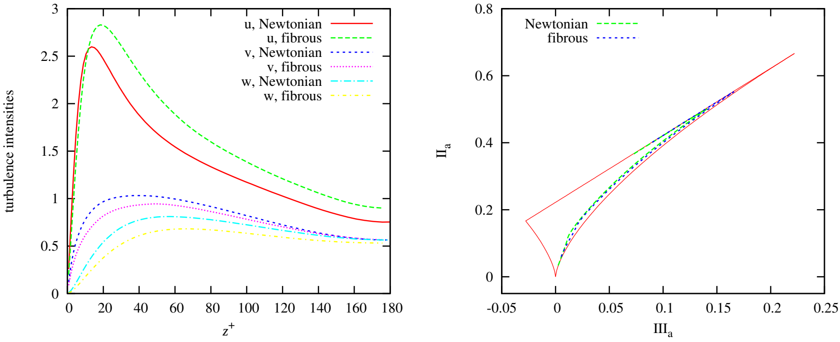

# Shear stress balance in wall-normal direction

$$\mu \frac{\mathrm{d}\langle U\rangle}{\mathrm{d}z} - \rho\langle uw\rangle + \left\langle \tau_{xz}^{\mathrm{NN}}\right\rangle = \tau_w + \frac{\mathrm{d}\langle p\rangle}{\mathrm{d}x}\, z$$

$DR = 16\%, \quad DR_{hyb} = 18.5\%, \quad DR_{IBOF} = 13.4\%$

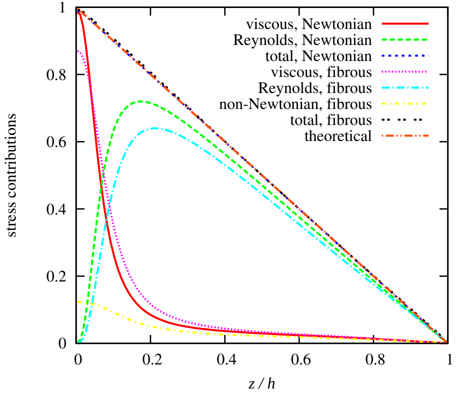

# Summary

- Developing a two-way coupled algorithm for direct simulation of turbulent drag reduction by rigid fibers
- Requires no closure model
- DNS of a drag-reduced turbulent channel flow at $Re_\tau = 180$
- Predicted DR $= 16\%$ lies between the predictions of hybrid and IBOF closure models

# Acknowledgments

We acknowledge

- International Graduate School of Science and Engineering (IGSSE) at Technische Universität München for financial support of this project.
- Leibniz Supercomputing Center (LRZ) in München for providing computing facilities.

Thanks for your attention.